

In Situ Preparation, Characterization, and Catalytic Application of Various Amine Functionalized Microporous SAPO-37

Maqsood Ahmed¹, Rekha Yadav¹, and Ayyamperumal Sakthivel^{1, 2, *}

¹Department of Chemistry, Inorganic Materials and Catalysis Laboratory, University of Delhi (North Campus) Delhi 110007, India

²Central University of Kerala, Reverside Transit Campus Padnekkad, Nileshwar, Kasaragod District 671314, Kerala, India

A series of monoamine, diamine, and aniline functionalized microporous silicoaluminophosphate molecular sieves (SAPO-37) was prepared by introduction of organo-silane ligand during hydrothermal synthesis. The template was selectively removed by the solvent extraction method in the presence of sodium nitrate salt. The effective removal of the template was evident from FT-IR, and ¹³C MAS-NMR studies. The retention of high crystallinity was evident from the powder XRD pattern of the template-removed functionalized SAPO-37 materials. The functionalized materials showed a high surface area in the range of 200–300 m²g⁻¹ with a pore volume of 0.2–0.4 cm³g⁻¹. The functionalized SAPO-37 was found to be a potential catalyst for epoxide ring opening with aniline.

Keywords: Amine-Functionalization, SAPO-37, Microporous Materials, Epoxide Ring Opening.

Copyright: American Scientific Publishers
Delivered by Ingenta

1. INTRODUCTION

Zeolites and zeolite-like molecular sieves are emerging materials for various catalytic and adsorption processes in the petroleum and petrochemical industries.^{1–3} In particular, faujasite (FAU)-type zeolite, viz., zeolite-Y having a 3D channel system with a 12-membered pore opening, is known as a potential catalyst in fluid catalytic cracking (FCC) and crude oil industry.⁴ Microporous silicoaluminophosphate SAPO-37 is analogous to the faujasite-type zeolite-Y structure, but it has been explored relatively less compared to zeolite-Y owing to its poor structural stability in the presence of moisture.^{5–7} In this regard, surface functionalization of these materials with different organosilanes might facilitate the generation of a hydrophobic environment and may also potential catalyst and adsorbents. The introduction of organosilane into mesoporous silica based molecular sieves has been widely investigated.^{8–15} Generally the surface functionalization of molecular sieves can be achieved through two different approaches: either the post-synthesis grafting method (*ex-situ* synthesis) or the direct co-condensation method (*in situ* synthesis).^{16–18} The post-synthesis grafting method has been extensively utilized for mesoporous

materials and further, the functionalized mesoporous materials have been explored for various applications such as metal ion capture,⁸ CO₂ capture,^{19–21} and base-catalyzed organic transformations.^{22–29} However, there are only limited reports on the surface functionalization of microporous molecular sieve materials.^{17–22} Incorporation of organosilane into the framework of faujasite-type silicoaluminophosphate (SAPO-37) via a direct co-condensation method can enhance its surface hydrophobicity, which may also help to improve its structural stability and catalytic activities. It is worth mentioning here that in comparison to post-synthesis functionalization, the direct co-condensation method or *in situ* synthesis involves the uniform distribution of organosilane moiety in the channels of framework surfaces.^{8, 29} These organosilane moieties can be covalently connected to the framework tetrahedral sites T (T = Si, P, or Al) through an Si–O–T bond. Herein we report the preparation of a series of organosilanes viz. (3-aminopropyl)triethoxysilane, *N*-[3-(triethoxysilyl)propyl]ethylenediamine, and *N*-[3-(Trimethoxysilyl)propyl]aniline containing faujasite-type SAPO-37 molecular sieves by the co-condensation method. The templates present in the as-prepared materials were efficiently removed through the solvent extraction method using ethanolic sodium nitrate solution. Unlike

*Author to whom correspondence should be addressed.

extraction with mineral acids such as HCl, which leads to the leaching of framework aluminium, the sodium nitrate solution effectively removed the template from microporous silicoaluminophosphate without dealumination. The resultant extracted microporous SAPO-37 samples were studied for β -amino alcohol preparation by propylene oxide ring opening with aniline under solvent-free conditions under ambient conditions.

2. EXPERIMENTAL SECTION

2.1. Chemicals

Pseudoboehmite (76% Al_2O_3 ; ACE, India), fumed silica (Aerosil-200), (3-aminopropyl)triethoxysilane, *N*-[3-(triethoxysilyl)propyl]ethylenediamine, and *N*-[3-(trimethoxysilyl)propyl]aniline were purchased from Sigma Aldrich, *ortho*-phosphoric acid (H_3PO_4 ; 85%) was received from Merck. Aqueous solution of tetramethylammonium hydroxide (25 wt%; TMAOH), aqueous solution of tetrapropylammonium hydroxide (40 wt%; TPAOH; Tritech Chemicals), Aniline (99% from CDH),

Propylene oxide (99% from Spectrochem) were used as received form.

2.2. Preparation of Functionalized SAPO-37

SAPO-37 with different aminosilane functionalities was prepared under hydrothermal conditions by the co-condensation method. In a typical procedure, first SAPO-37 precursor was prepared by using a molar gel composition of 1.0 $(\text{TPA})_2\text{O}$:0.025 $(\text{TMA})_2\text{O}$:1.0 Al_2O_3 :1.0 P_2O_5 :0.43 SiO_2 :50 H_2O .^{30–32} About 5.25 g of pseudoboehmite was dissolved in diluted orthophosphoric acid and aged for 12 h while stirring, and the resulting mixture was called solution A. Another solution (B) was prepared by adding a calculated amount (1.03 g) of fumed silica into a mixture containing 40.5 g of TPAOH (40 wt% in H_2O) and 0.73 g of TMAOH (25 wt% in H_2O). Solution B was added into solution A with continuous stirring and subsequently stirred overnight at room temperature. The resultant synthesis gel was crystallized for 8 h at 200 °C in a Teflon-lined autoclave to obtain SAPO-37 precursor. A known amount of

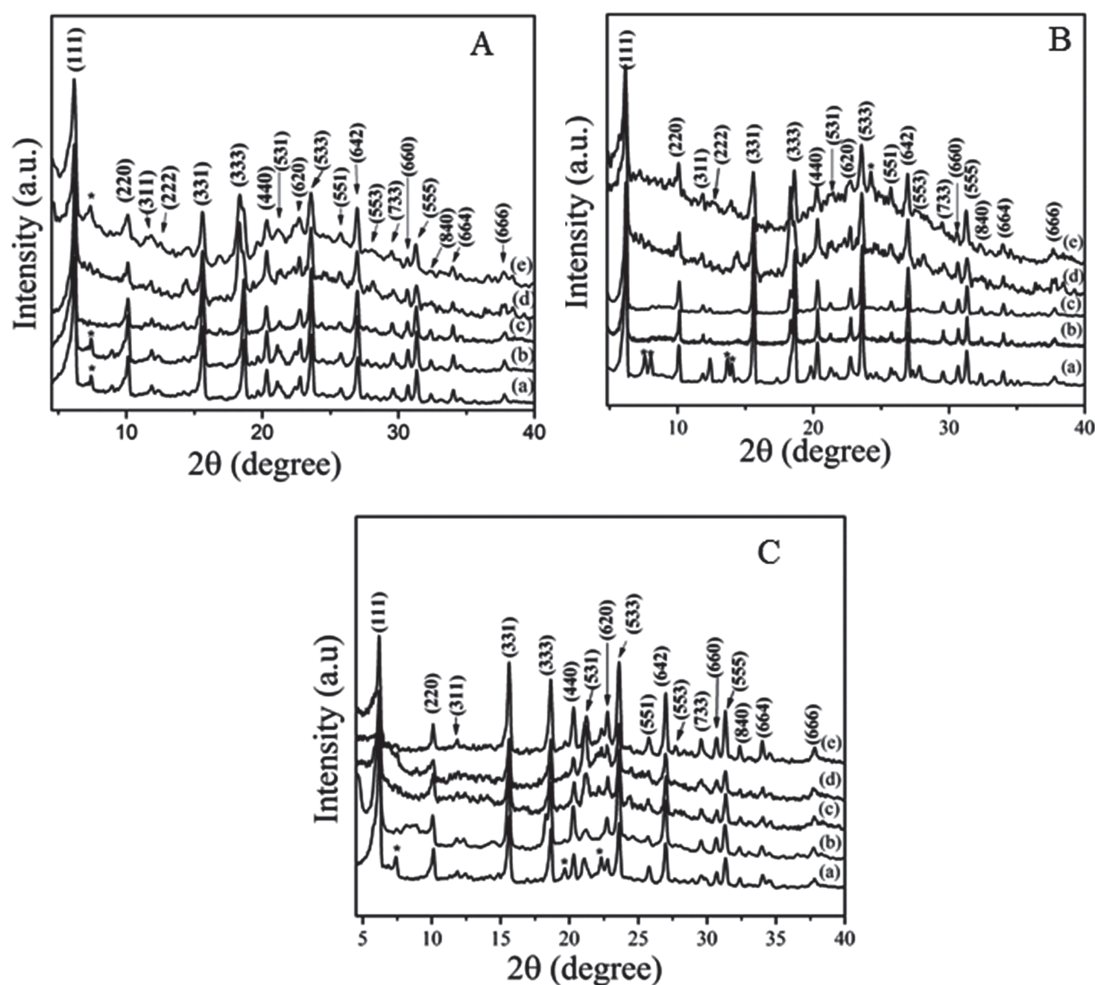


Figure 1. Powder XRD pattern of as-prepared SAPO-37-*x*N (A), SAPO-37-*x*NN (B) and SAPO-37-*x*AN (C) (where *x* = 0.04 (a), 0.16 (b), 0.24 (c), 0.32 (d) and 0.40 (e)).

organosilane, for example (3-aminopropyl)triethoxysilane, was added to the above-prepared SAPO-37 precursor and the resulting gel was allowed to crystallize for 16 h at 200 °C. The obtained amino silane functionalized SAPO-37 materials were filtered, washed with ethanolic water, and dried in an air oven at 80 °C. An identical procedure was followed for the preparation of SAPO-37 with *N*-[3-(triethoxysilyl)propyl]ethylenediamine and *N*-[3-(trimethoxysilyl)propyl]aniline. The samples prepared using (3-aminopropyl)triethoxysilane, *N*-[3-(triethoxysilyl)propyl]ethylenediamine, and *N*-[3-(trimethoxysilyl)propyl]aniline are denoted as SAPO-37-*x*N, SAPO-37-*x*NN, and SAPO-37-*x*AN respectively (where *x* ranges from 0.04 to 0.40 M) with respect to the above molar composition. The templates present in the as-synthesized materials were removed by a novel solvent extraction method by refluxing about 1 g of sample in 100 ml of ethanol (EtOH) containing 0.3 g of sodium nitrate at 80 °C for 6 h. The final extracted samples were denoted as SAPO-37-*x*N-ex, SAPO-37-*x*NN-ex, and SAPO-37-*x*AN-ex, respectively.

2.3. Characterization Methods

Powder X-ray diffraction patterns of all the materials were collected on Brüker-D8 high resolution X-ray

diffractometer with Cu-K α radiation ($\lambda = 1.5418 \text{ \AA}$), between 2θ range of 4–40°, with a scan speed and step size of 0.5°/min and 0.02° respectively. FT-IR spectra were measured on Brüker optic model tensor 27 FT-IR spectrometer in the range of 400–4000 cm^{-1} using KBr methods. Solid-state NMR experiments were carried out on a Bruker AVANCE 400 wide bore spectrometer equipped with a superconducting magnet with a field of 7.1 T using a 4 mm double resonance magic angle spinning (MAS) probe operating at resonating frequencies of 79.4, and 104.26 MHz for ^{29}Si , and ^{13}C respectively. The samples were packed in 4 mm zirconia rotors and subjected to a spinning speed of 10 kHz: single pulse experiment with pulse duration of 4.5 μs and a relaxation delay time of 6 s were used for recording all ^{29}Si , and ^{13}C MAS NMR patterns. All chemical shift values are expressed with respect to 2,2-dimethyl-2-silapentane-5-sulfonate sodium salt (DSS) for the ^{29}Si and ^{13}C nucleus. The morphology of the materials was studied using scanning electron microscopy (SEM, JEOL, JSM 6610 LV with gold sputter coater JEC 300). Nitrogen adsorption/desorption isotherms were recorded on Micromeritics ASAP 2020, USA. The samples were degassed at 250 °C for 12–14 h under 0.1333 Pascal pressure and analysis was carried out at –196 °C prior to each analysis. The BET surface

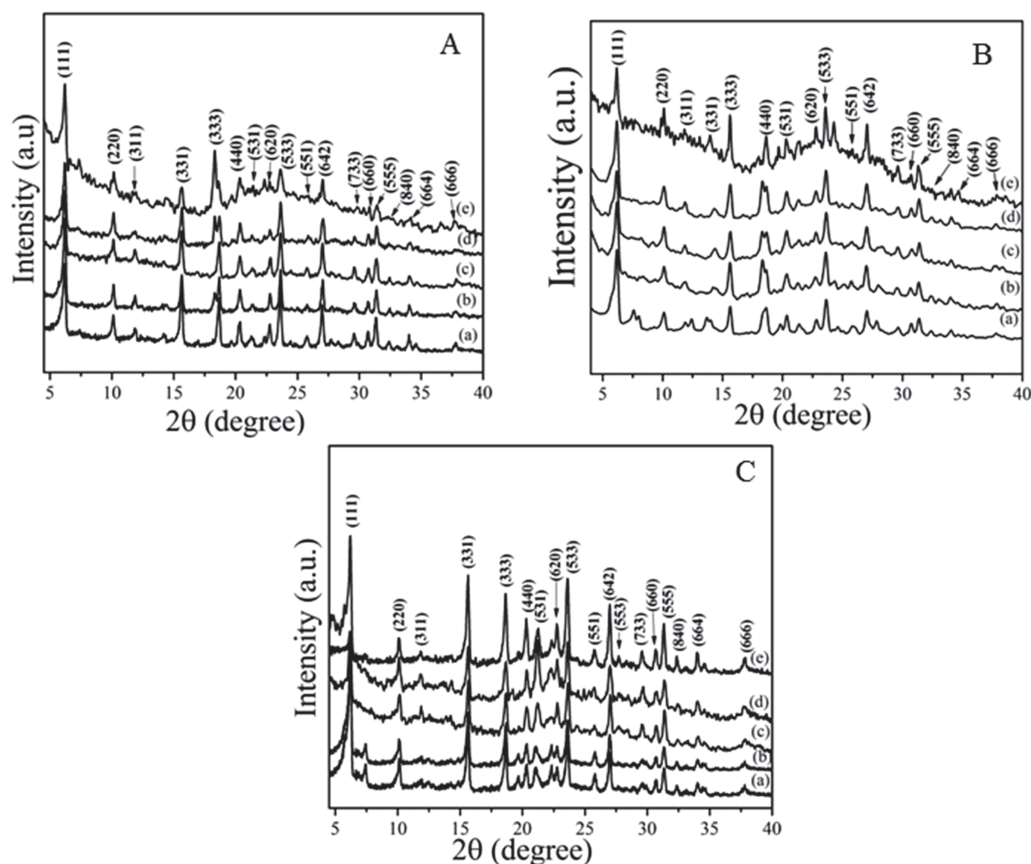


Figure 2. Powder XRD pattern of extracted SAPO-37-*x*N-ex (A), SAPO-37-*x*NN-ex (B) and SAPO-37-*x*AN-ex (C) (where *x* = 0.04 (a), 0.16 (b), 0.24 (c), 0.32 (d) and 0.40 (e)).

area was calculated in the relative pressure range (p/p_0) 0.05–0.3, over the adsorption branch of the isotherm. The soluble basicity of the functionalized SAPO-37 was determined by argentometric titration using 0.1 N AgNO_3 .³³ In particular procedure 500 mg of sample was treated with 5.21 g of 35 wt% HCl in 50 ml EtOH for 2 h followed by 2–3 times washing with ethanol and then dried to remove the excess of HCl. Then with 4.6 g of 69 wt% HNO_3 in 50 ml ethanol was added to the dried sample and stirred for 2 hours. The solid was filtered and washed very well with EtOH. Both the filtrate and washing were combined and treated with 50 ml of 0.1 N solution of AgNO_3 under stirring condition. The formed precipitate of AgCl was filtered washed and then dried under dark condition prior to weighing the precipitate.

2.4. Catalytic Studies on Epoxide Ring Opening

The catalytic activities of the extracted organo-functionalized SAPO-37 materials were investigated for the ring opening of propylene oxide with aniline to get β -amino alcohol. The procedure involve by taking

10.7 mmol of aniline and 16.0 mmol of propylene oxide in a round bottom flask having 100 mg of functionalized SAPO-37 catalyst. The resulting mixture was stirred for 7 h at 35 °C. After reaction the products were separated by dissolving a calculated amount of toluene followed by filtration. The separated products were analyzed using gas chromatography (GC) with FID detector. Further the products were confirmed through GC-MS and subsequently by ^1H and ^{13}C NMR spectra after isolation through column chromatography. The GC-MAS results were consistent with the molecular weight of the isolated products. The filtered catalyst was washed with ethanol and reused after dried at 80 °C.

3. RESULTS AND DISCUSSION

Figure 1 shows the powder XRD patterns for all the as-synthesized samples of SAPO-37, SAPO-37- $x\text{N}$, SAPO-37- $x\text{NN}$, and SAPO-37- $x\text{AN}$ ($x = 0.04, 0.16, 0.24, 0.32,$ and 0.40) which exhibited well-resolved reflections characteristic of faujasite-type SAPO-37 framework structure.^{30–32,34} The crystallinity of the materials was

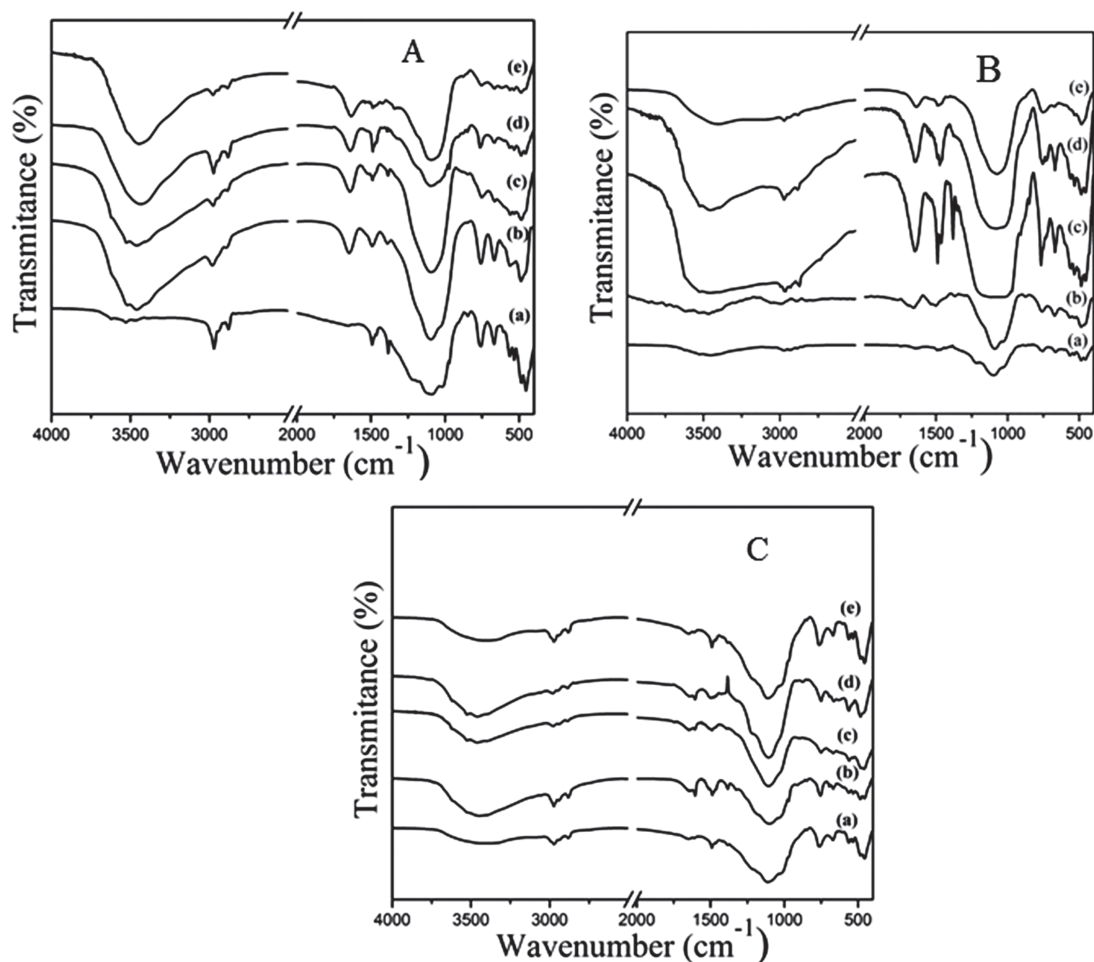


Figure 3. FT-IR spectra of as-prepared SAPO-37- $x\text{N}$ (A), SAPO-37- $x\text{NN}$ (B) and SAPO-37- $x\text{AN}$ (C) (where $x = 0.04$ (a), 0.16 (b), 0.24 (c), 0.32 (d) and 0.40 (e)).

retained even at higher concentrations of organosilane loading. Additional very weak reflections that were evident on samples prepared using relatively low organosilane functionality at 2θ of around 8 and 21 could be from the conversion of SAPO-37 into AFI-type SAPO-5 phase. The powder XRD patterns of the solvent extracted various organosilane functionalized SAPO-37 is shown in Figure 2. All the samples retained the reflection characteristics of the faujasite phase with relative broadening of the peaks due to the presence of the functional group on the framework sites. It is worth mentioning here that, unlike literature reports where the SAPO-37 structure converted to amorphous phase after removing template, in the present studies samples retains high crystallinity even after template removed by extraction. The above fact supports the proposal that the organosilane functionality present in the framework facilitates stabilization of the SAPO-37 framework structures.

The FT-IR spectra of functionalized SAPO-37 materials obtained with different amines (monoamine, diamine, and aniline) are shown in Figure 3. All the samples

showed framework secondary-building-unit (SBU) vibrational bands at around 561 and 535 cm^{-1} , corresponding to the double-six membered (D6R) faujasite structure of SAPO-37. The functionalized materials showed additional vibration bands at 1487 and 1560 cm^{-1} , which are attributed to the bending vibration of the NH and NH_2 functionality present in organosilane-functionalized SAPO-37 framework. The intense band in the region of 1108 cm^{-1} corresponds to the asymmetric stretching of T-O-T (T = Si, Al, and P). The presence of CH_2 groups derived from the linker moiety of organosilane was evident from stretching vibration bands that appeared in the range of 2700–3000 cm^{-1} . All of the template-extracted samples showed drastic decreases in the intensity of the vibrational band that appeared around 2700–3000 cm^{-1} (Fig. 4), suggesting the effective removal of template from the functionalized SAPO-37 framework. However, the functionalized SAPO-37 retained the bending vibration bands at around 1487 and 1560 cm^{-1} , clearly suggesting that amine functionalities are retained on the framework sites after template extraction.

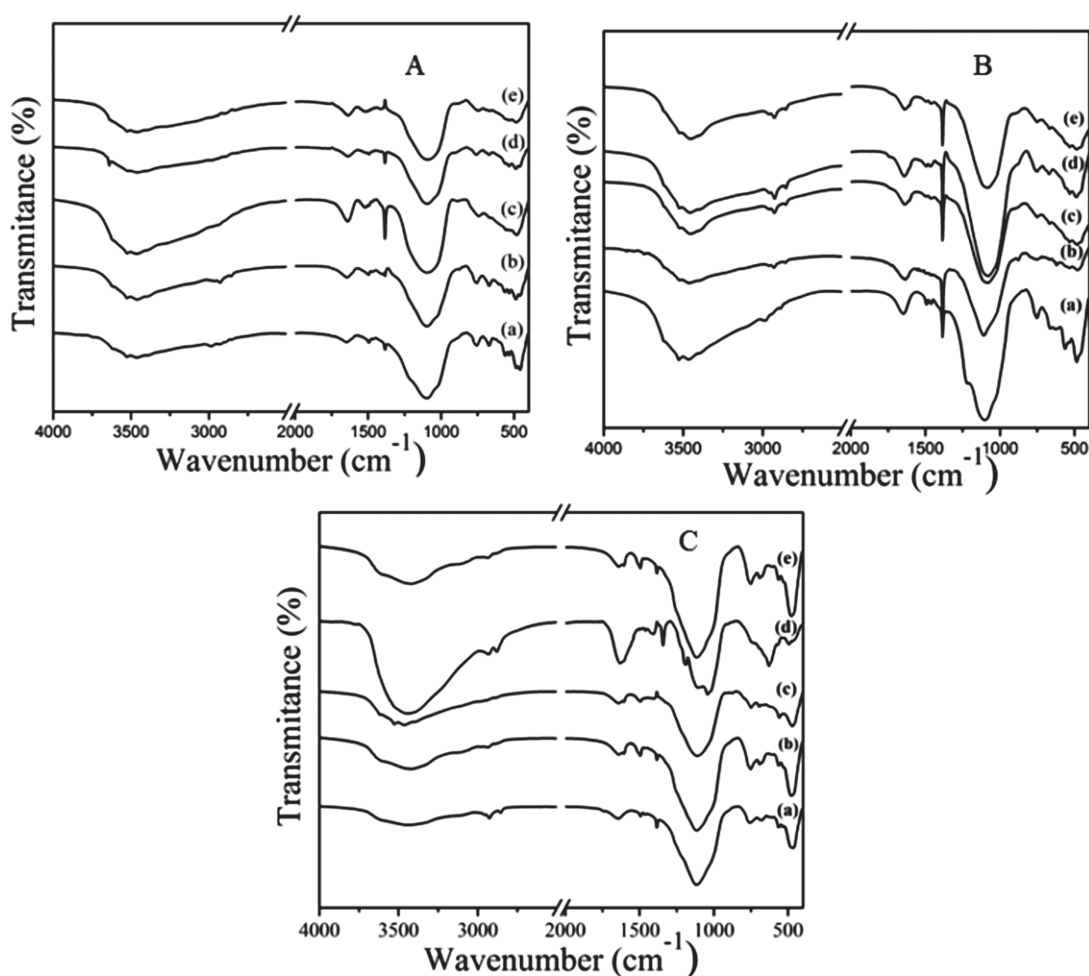


Figure 4. FT-IR spectra of extracted SAPO-37- x N-ex (A), SAPO-37- x NN-ex (B) and SAPO-37- x AN-ex (C) (where $x = 0.04$ (a), 0.16 (b), 0.24 (c), 0.32 (d) and 0.40 (e)).

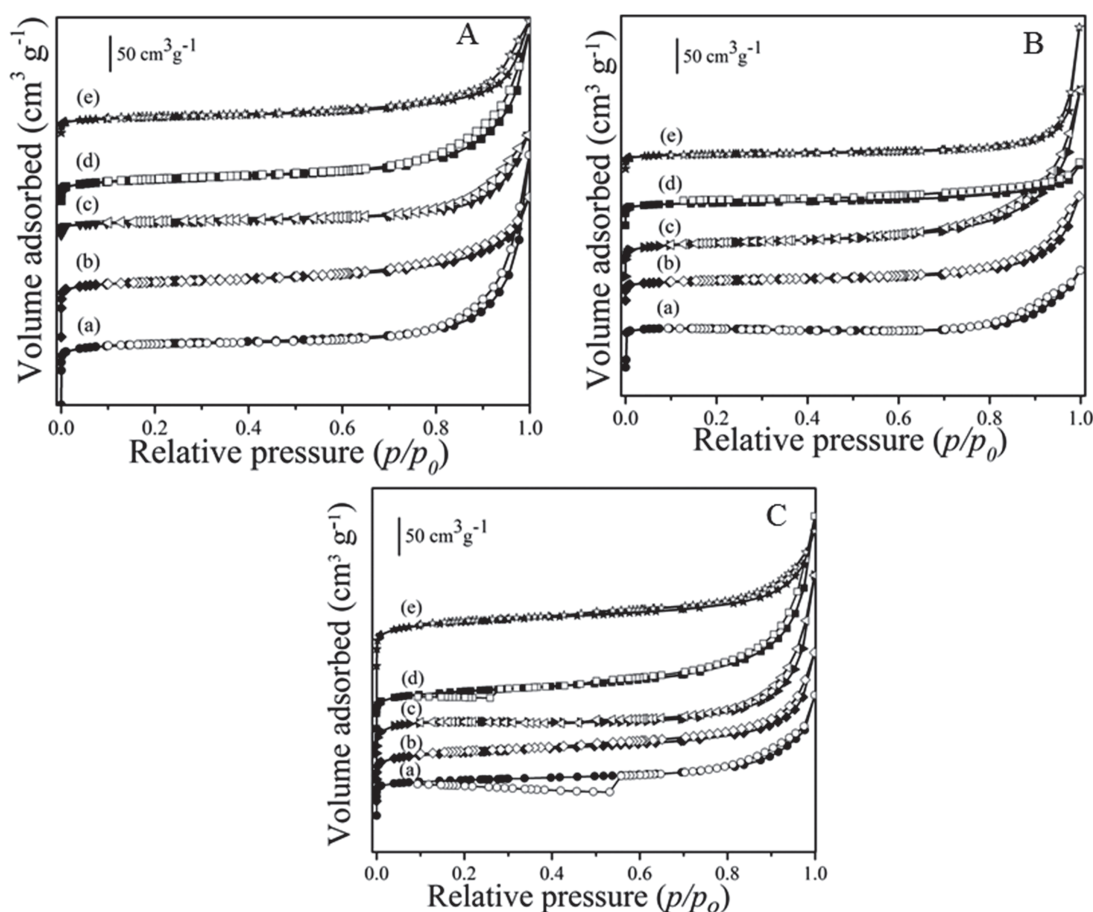


Figure 5. N_2 sorption of extracted SAPO-37- x N-ex (A), SAPO-37- x NN-ex (B) and SAPO-37- x AN-ex (C) (where $x = 0.04$ (a), 0.16 (b), 0.24 (c), 0.32 (d) and 0.40 (e)).

The N_2 sorption isotherms of template-extracted SAPO-37- x N-ex, SAPO-37- x NN-ex, and SAPO-37- x AN-ex ($x = 0.04, 0.16, 0.24, 0.32$ and 0.40) obtained using different concentrations of organosilane ligands are shown in Figure 5. The textural properties, such as the BET surface area (S_{BET}), micropore surface area (S_p), micropore volume (V_p), and total pore volume are summarized in Table I. The isotherms of all the extracted samples are typical of type I with a sharp uptake in the relative pressure (p/p_0) region below 0.1. The increase in concentration of the functional group on SAPO-37 results in decreases in the surface area and pore volume, which are evident in the case of SAPO-37- x N-ex, and SAPO-37- x NN-ex materials. However, in the case of SAPO-37- x AN-ex, an increase in propyl-aniline functionality facilitates an increase in the surface area, might be due to the presence of heavy organic (aniline) functional moiety, which has difficulty fitting into the framework sites. Thus propyl-aniline silane partially condensed on the external framework sites, which generated hierarchical pores after template extraction, as is evident from the hysteresis in the N_2 sorption isotherm as well as the surface roughness evident from SEM analysis.

The incorporation of organosilane into the framework of SAPO-37 was investigated by ^{29}Si and ^{13}C MAS NMR spectra. ^{29}Si MAS NMR spectra of functionalized SAPO-37 obtained from different organosilane functional

Table I. Textural properties of extracted SAPO-37- x N-ex, SAPO-37- x NN-ex and SAPO-37- x AN-ex samples.

Samples	Surface area (m^2g^{-1})		Volume (cm^3g^{-1})		Amine contents mmol (N) g^{-1}
	Micropore surface area	S_{BET}	Micropore volume	Total volume	
SAPO-37-0.04N-ex	219.9	277.3	0.11	0.56	0.24
SAPO-37-0.16N-ex	187.9	252.6	0.09	0.31	–
SAPO-37-0.24N-ex	42.0	112.8	0.02	0.37	0.69
SAPO-37-0.32N-ex	27.4	84.4	0.01	0.31	1.05
SAPO-37-0.40N-ex	34.6	87.7	0.01	0.31	1.46
SAPO-37-0.04NN-ex	220.0	202.0	0.11	0.26	0.25
SAPO-37-0.16NN-ex	174.2	219.6	0.08	0.25	1.46
SAPO-37-0.24NN-ex	114.3	188.0	0.05	0.50	1.67
SAPO-37-0.32NN-ex	88.5	123.9	0.04	0.16	2.05
SAPO-37-0.40NN-ex	47.6	82.8	0.02	0.38	–
SAPO-37-0.04AN-ex	200.1	287.0	0.10	0.47	0.30
SAPO-37-0.16AN-ex	131.7	212.5	0.06	0.31	1.00
SAPO-37-0.24AN-ex	222.7	239.9	0.11	0.43	1.46
SAPO-37-0.32AN-ex	111.4	241.5	0.05	0.65	1.80
SAPO-37-0.40AN-ex	263.8	362.3	0.13	0.37	1.77

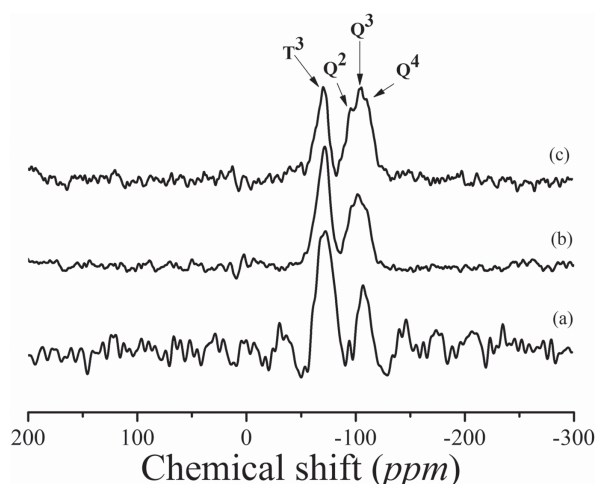


Figure 6. ^{29}Si MAS NMR of SAPO-37-0.16N-ex (a), SAPO-37-0.16NN-ex (b) and SAPO-37-0.16AN-ex (c).

groups such as SAPO-37-0.16N-ex, SAPO-37-0.16NN-ex, and SAPO-37-0.16AN-ex are shown in Figure 6. All the samples showed peaks at around -96 , -105 , and -110 ppm, corresponding to Si (3Al, Si), Si (2Al, 2Si), and Si (0Al, 4Si) environments.^{35,36} An additional peak with strong intensity appeared at around -70 ppm, which corresponds to condensed silicon in an organosilane environment (T^3 sites), clearly supporting the presence of an organo-functional group covalently bonded on the surface of SAPO-37 framework. The ^{13}C MAS NMR spectra of SAPO-37-0.16N-ex, SAPO-37-0.16NN-ex, and SAPO-37-0.16AN-ex showed intense peaks at 10, 20, and 44 ppm, which were derived from the propyl linker moiety present in functionalized SAPO-37 (Fig. 7). Two additional peaks were evident on SAPO-37-0.16NN-ex at 36.5 and 50.2 ppm, corresponding to the ethylene moiety of the

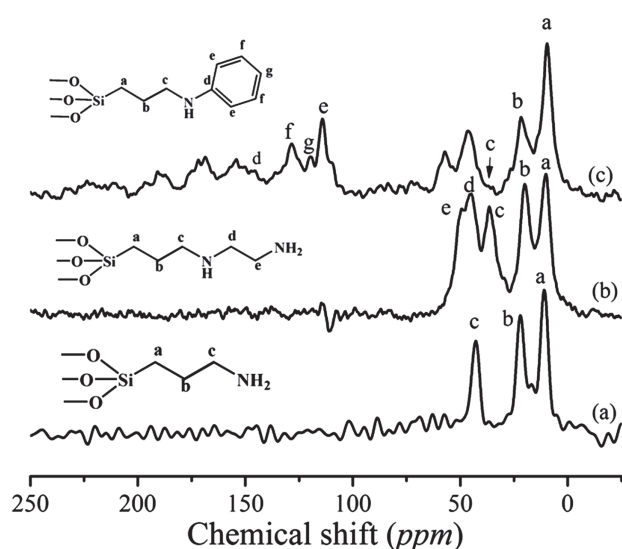


Figure 7. ^{13}C MAS NMR spectra of SAPO-37-0.16N-ex (a), SAPO-37-0.16NN-ex (b) SAPO-37-0.16AN-ex (c).

propyl-ethylene-diamino silane linker. Similarly, SAPO-37-0.16AN-ex showed additional peaks at around 117 and 134 ppm derived from the aromatic ring of the aniline-propyl-silane moiety. It is evident from the ^{13}C MAS NMR studies that organo-functionality is present in the SAPO-37 framework, which is in agreement with FT-IR studies.

The external morphologies of the SAPO-37 functionalized with different organosilanes were studied through SEM. The SEM images (Fig. 8) of SAPO-37 with different organosilane functionalized SAPO-37 materials possessing different concentrations of silane showed typically octahedral morphology of faujasite structure with high crystallinity. The surface roughness increased with increasing concentration of organo-functional silane. The shape and size of the particles changed when the concentration of organosilanes was varied.

Thoroughly characterized organo-functionalized SAPO-37 was studied for base-catalyzed ring opening of propylene oxide with aniline under solvent-free conditions (Scheme 1). The 1-(phenylamino)propan-2-ol (c) and 2-(phenylamino)propan-1-ol (d) were obtained as the major product with small amount of di-alkylated aniline (Scheme 1). The fractional amount of dialkylated aniline with tertiary amine groups was either formed directly from (a) or from regioisomers (c) or (d). The products were separated by column chromatography and confirmed by ^1H and ^{13}C NMR spectra. All of the reactions were carried out with an aniline-to-propylene oxide molar ratio of 1:1.5 at 35°C for 7 h. The conversion was calculated with respect

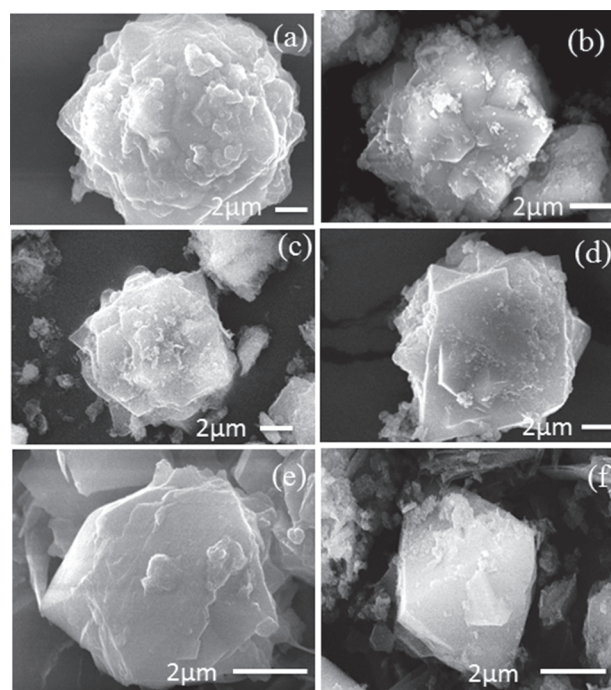
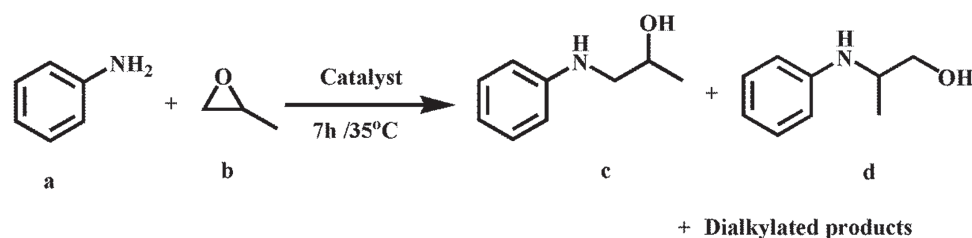


Figure 8. SEM images of as-prepared SAPO-37-0.04N (a), SAPO-37-0.40N (b), SAPO-37-0.04NN (c), SAPO-37-0.32NN (d), SAPO-37-0.04AN (e) and SAPO-37-0.40AN (f) (Scale represents $2\ \mu\text{m}$).



Scheme 1. Pictorial representation of propylene oxide ring opening with aniline.

Table II. Catalytic behavior of functionalized SAPO-37 for epoxide ring opening with aniline.

Catalyst	Conversion (%)	Selectivity (%)	
		Mono-alkylated	Di-alkylated
SAPO-37-0.04N-ex	57.3	86.4	13.6
SAPO-37-0.16N-ex	81.2	73.8	26.2
SAPO-37-0.24N-ex	71.9	80	20.0
SAPO-37-0.32N-ex	64.2	84.2	15.8
SAPO-37-0.40N-ex	20.7	92.9	7.10
SAPO-37-0.04NN-ex	54.5	86.8	13.2
SAPO-37-0.16NN-ex	78.4	81.8	16.7
SAPO-37-0.24NN-ex	71.9	80.2	19.8
SAPO-37-0.32NN-ex	38.0	92.7	7.3
SAPO-37-0.40NN-ex	14.0	98.6	1.4
SAPO-37-0.04AN-ex	58.3	86.5	13.5
SAPO-37-0.16AN-ex	71.9	80	20
SAPO-37-0.24AN-ex	85.0	70.8	29.2
SAPO-37-0.32AN-ex	69.5	82.5	17.5
SAPO-37-0.40AN-ex	69.6	84.9	15.1

to aniline by gas chromatography. The catalytic data for all the samples (viz. SAPO-37-*x*N-ex, SAPO-37-*x*NN-ex, and SAPO-37-*x*AN-ex, with *x* = 0.04, 0.16, 0.24, 0.32, and 0.40) are summarized in Table II. It is clear from the table that the conversion of aniline increases with the amine concentration present in the catalyst increases from 0.04 to 0.24 and reaches the maximum conversion when the catalyst have an amine functionality concentration in the range of 0.16 or 0.24. A further increase in amine concentration, a decrease in conversion was evident which might be due to decrease in surface area and surface exposed active sites. In the case of SAPO-37-*x*AN-ex, the catalytic conversion remains identical; this might be due to the presence of aniline functional group on the external surface of the SAPO-37 framework, which was evident from surface area analysis, in which the SAPO-37-0.40AN-ex sample showed the maximum surface area. The catalytic activity remained intact after several recycling runs.

4. CONCLUSION

First time a series of monoamine, diamine and aniline organo-functional groups were incorporated into the SAPO-37 framework by co-condensation method. The presence of -NH and -NH₂ functionality was evident from FT-IR and ¹³C-MAS NMR studies. The covalent grafting of organo-functional group was evident from ²⁹Si-MAS

NMR and ¹³C-MAS NMR spectra. The powder XRD pattern of templated extracted samples retained faujasite type SAPO-37 structure. The introduction of aniline silane functionality enhances the surface area owing to the presence of hierarchical pore. The functionalized materials were shown as promising catalysts for epoxide ring opening at ambient conditions.

Acknowledgments: Authors express their sincere thanks to DST-SERB (EMR/2014/001214) India, for their financial support. Authors are also thankful to USIC, University of Delhi, for the support on instrumentation facility and Dr. R. Nagarajan, University of Delhi for his support on use of powder XRD facility under DST (Nano Mission). Maqsood Ahmed and Rekha Yadav are grateful to CSIR and UGC, India for their research fellowship respectively.

References and Notes

- R. Yadav and A. Sakthivel, *Appl. Catal. A Gen.* 481, 143 (2014).
- W. Vermeiren and J. P. Gilson, *Top Catal.* 52, 1131 (2009).
- A. Corma, M. J. Díaz-Cabañas, J. M. Triguero, F. Rey, and J. Rius, *Nature Mater.* 418, 514 (2002).
- G. Busca, *Chem. Rev.* 107, 5366 (2007).
- J. A. Martens, P. J. Grobet, and P. A. Jacobs, *J. Catal.* 126, 299 (1990).
- B. L. Su and D. Barthomeuf, *J. Catal.* 139, 81 (1993).
- G. Fernandes and V. Fernandes, *Catal. Today* 75, 233 (2002).
- T. Yokoi, H. Yoshitake, and T. Tatsumi, *J. Mater. Chem.* 14, 951 (2004).
- X. S. Zhao and G. Q. Lu, *J. Phys. Chem. B* 102, 1556 (1998).
- K. Ariga, Y. Yamauchi, G. Rydzek, Q. Ji, Y. Yonamine, K. C. W. Wu, and J. P. Hill, *Chem. Lett.* 43, 36 (2014).
- V. Malgras, Q. Ji, Y. Kamachi, T. Mori, F. Shieh, K. C. W. Wu, K. Ariga, and Y. Yamauchi, *Bull. Chem. Soc. Jpn.* 88, 1171 (2015).
- W. Nakanishi, K. Minami, L. K. Shrestha, Q. Ji, J. P. Hill, and K. Ariga, *Nano Today* 9, 378 (2014).
- K. Ariga, T. Mori, S. Ishihara, K. Kawakami, and J. P. Hill, *Chem. Mater.* 26, 519 (2014).
- A. Vinu, K. Z. Hossain, and K. Ariga, *J. Nanosci. Nanotechnol.* 25, 347 (2005).
- R. Kotsilkova, E. Ivanov, and V. Michailova, *Nanosci. Nanotechnol. Lett.* 8, 1056 (2012).
- J. A. Melero, R. V. Grieken, and G. Morales, *Chem. Rev.* 106, 3790 (2006).
- L. H. Hsiao, S. Y. Chen, S. J. Huang, S. B. Liu, P. H. Chen, J. C. Chan, and S. Cheng, *Appl. Catal. A* 359, 96 (2009).
- S. Shylesh and A. R. Sing, *J. Catal.* 244, 52 (2006).
- J. Y. Kim, J. Kim, S. T. Yang, and W. S. Ahn, *Fuel* 108, 515 (2013).
- M. U. M. Junaidi, C. P. Khoo, C. P. Leo, and A. L. Ahmad, *Microporous Mesoporous Mater.* 192, 52 (2014).
- Y. Belmabkhout and A. Sayari, *Adsorption* 15, 318 (2009).

22. K. Ariga, M. Pumera, and M. Aono, *Sci. Tech. Adv. Mater.* 6, 10302 (2015).
23. T. Yokoi, H. Yoshitake, T. Yamada, Y. Kubotac, and T. Tatsumi, *J. Mater. Chem.* 16, 1125 (2006).
24. N. L. Torad, M. Hu, S. Ishihara, H. Sukegawa, A. A. Belik, M. Imura, K. Ariga, Y. Sakka, and Y. Yamauchi, *Small* 10, 2096 (2014).
25. X. Wang, Y. H. Tseng, J. C. C. Chan, and S. Cheng, *Microporous Mesoporous Mater.* 85, 241 (2005); 95, 57 (2006).
26. R. Yadav, M. Ahmed, A. K. Singh, and A. Sakthivel, *Scientific Reports* (2016), DOI No: 10.1038/srep 22813.
27. Sujandi, S. E. Park, D. S. Han, S. C. Han, M. J. Jin, and T. Ohsuna, *Chem. Commun.* 39, 4131 (2006).
28. S. Saravanamurugan, Sujandi, D. S. Han, J. B. Koo, and S. E. Park, *Catal. Commun.* 9, 158 (2008).
29. X. Wang, K. S. K. Lin, J. C. C. Chan, and S. Cheng, *J. Phys. Chem. B* 109, 1763 (2005).
30. L. S. de Saldarriaga, C. Saldarriaga, and M. E. Davis, *J. Am. Chem. Soc.* 109, 2686 (1987).
31. R. Yadav, A. K. Singh, and A. Sakthivel, *Chem. Lett.* 42, 1160 (2013).
32. R. Yadav, A. K. Singh, and A. Sakthivel, *Catal. Today* 245, 155 (2015).
33. A. B. Bourlinos, T. Karakostas, and D. Petridis, *J. Phys. Chem B* 107, 920 (2003).
34. L. Zhang, D. Chen, H. Y. Nie, and Y. Huang, *Microporous and Mesoporous Mater.* 175, 147 (2013).
35. C. S. Blackwell and R. D. Patton, *J. Phys. Chem.* 92, 3965 (1988).
36. A. K. Singh, K. Kondamudi, R. Yadav, S. Upadhyayula, and A. Sakthivel, *J. Phys. Chem C* 118, 27961 (2014).

Received: 18 December 2015. Accepted: 30 January 2016.

IP: 91.204.15.102 On: Fri, 26 Oct 2018 16:24:59
Copyright: American Scientific Publishers
Delivered by Ingenta